

Clinical Applications of Diffusion-Weighted-MRI in Prostate Cancer

Pornphan Wibulpolprasert MD*,
Sith Phongkitkarun MD*, Panas Chalermpanyakorn MD**

* Department of Diagnostic and Therapeutic Radiology, Faculty of Medicine, Ramathibodi Hospital,
Mahidol University, Bangkok, Thailand

** Department of Pathology, Faculty of Medicine, Ramathibodi Hospital, Mahidol University, Bangkok, Thailand

Objective: To determine the relationship between the apparent diffusion coefficient (ADC) values calculated from diffusion-weighted (DW) MR imaging in different b values and tumor grading by Gleason scores of the peripheral zone prostate cancer.

Material and Method: Thirty-nine patients with prostate cancer who underwent pre-operative endorectal Diffusion-Weighted (DW) magnetic resonance (MR) imaging between March 2006 and March 2010 were included. Regions of interest (ROIs) were drawn on ADC maps at sites of visible tumor on DW images and ADC maps comparison to histopathology. Differentiation between ADC values of tumor and non-tumor areas were analyzed by using paired t-test and sign-test and between tumors grading were analyzed by using Wilcoxon rank-sum (Mann-Whitney) test and Kruskal-Wallis equality-of population rank test.

Results: The mean ADC of tumor is lower than non-tumor areas at all b-values. There is negative correlation between ADC value and tumor grading with statistical significance at $b = 1,000 \text{ sec/mm}^2$, between tumor grade I ($1.95 \times 10^{-3} \text{ mm}^2/\text{sec}$, $SD = 0.33$) and tumor grade II ($1.16 \times 10^{-3} \text{ mm}^2/\text{sec}$, $SD = 0.27$) ($p = 0.03$) and between tumor grade I and tumor grade III ($1.10 \times 10^{-3} \text{ mm}^2/\text{sec}$, $SD = 0.36$) ($p = 0.002$) and at $b = 2,000 \text{ sec/mm}^2$, between tumor grade I ($2.21 \times 10^{-3} \text{ mm}^2/\text{sec}$, $SD = 0.08$) and tumor grade II ($1.22 \times 10^{-3} \text{ mm}^2/\text{sec}$, $SD = 0.38$) ($p = 0.01$), and between tumor grade I and tumor grade III ($1.32 \times 10^{-3} \text{ mm}^2/\text{sec}$, $SD = 0.49$) ($p = 0.04$). There is no statistical significance difference between tumor grade II and grade III.

Conclusion: Tumor shows restricted diffusion with ADC value lower than non-tumor areas. There is a significant negative correlation between ADCs and tumor grading between low and intermediate grades and between low and high grades tumor at the $b = 1,000$ and $2,000 \text{ sec/mm}^2$. ADC maps may be a useful tool for non-invasive assessment of the aggressiveness of prostate cancers that are visible on MR images.

Keywords: Endorectal diffusion-weighted-MRI, ADC values, Prostate cancer, Gleason score

J Med Assoc Thai 2013; 96 (8): 967-75

Full text. e-Journal: <http://jmat.mat.or.th>

Prostate cancer is the fourth leading site of male cancer in Ramathibodi Hospital in 2008⁽¹⁾ and the fifth leading site of male cancer in National Cancer Institute in 2009⁽²⁾. According to the NCCN clinical practice guidelines version 1.2011 of prostate cancer and seventh Edition of the AJCC Cancer Staging Manual, the effectiveness of the various treatment options for prostate cancer and degree of recurrence risk depends on the extent of disease. The initial clinical staging including digital rectal examination, PSA value,

and Gleason score of tumor are used for initial clinical assessment for predict life expectancy and plan for further management. Over the past two decades, endorectal magnetic resonance (MR) imaging has emerged as a relatively accurate method of evaluating the local extent and aggressiveness of prostate cancer. However, wider implementation of this technology has been limited by concerns about false-positive and false-negative results and interobserver variability⁽³⁾.

MRI of prostate cancer with conventional T2-weighted image is predominantly limited to staging for the presence of extracapsular extension and seminal vesicle invasion⁽⁴⁾. However, the more recent application of functional MRI technique, including diffusion-weighted image (DWI), has the potential to expand the role of MRI to noninvasive characterization

Correspondence to:

Phongkitkarun S, Department of Diagnostic and Therapeutic Radiology, Faculty of Medicine, Ramathibodi Hospital, Mahidol University, Bangkok 10400, Thailand.

Phone: 0-2201-1212

Email: sith.bkk@gmail.com

of prostate cancer by providing more specific information regarding tumor localization, size, and aggressiveness⁽⁴⁻⁸⁾. In addition, tumor apparent diffusion coefficient (ADC) on DWI may be correlated with prostate cancer progression and may help to stratify patients who may benefit from radical treatment⁽⁹⁾.

Several recent studies have shown that DWI can help differentiate between malignant and benign prostatic tissue on the basis of lower ADC values of prostatic carcinoma compared with normal prostatic tissue⁽¹⁰⁻¹²⁾. In the normal population, the mean ADC values of the central and peripheral zones of the prostate gland are statistically different⁽¹³⁾. While, the histopathologic reference standard for reporting prostate cancer aggressiveness is the Gleason grading system. More aggressive tumors are associated with decreased 10-year-survival⁽¹⁴⁾, and increased likelihood of prostate cancer recurrence⁽¹⁵⁾. The purpose of this study was to determine the relationship between the apparent diffusion coefficient (ADC) values calculated from diffusion-weighted-images (DWI) at different b-values and tumor grading by Gleason score of peripheral zone prostate cancer from radical prostatectomy specimens.

Material and Method

Patients

This retrospective study was approved by institutional review board, which waived the requirement for patient informed consent. Fifty-four consecutive patients who underwent 1.5-T endorectal MR imaging followed by radical prostatectomy in Ramathibodi Hospital between March 1, 2006 and March 31, 2010 were enrolled. Fifteen patients were excluded from analysis because their Diffusion Weighted Images were unavailable for review. The final study population consisted of thirty-nine men. Patient age, underlying disease, serum prostate-specific antigen (PSA) level, indication for endorectal MRI, date and type of radical prostatectomy were reviewed from medical records. The location and extension of tumor and Gleason score of prostate cancer were reviewed by urological pathologist. The initial and adjuvant post-operative treatment and first PSA level after radical prostatectomy were also recorded.

MRI technique

All prostate MRI examinations were performed by using an endorectal coil (Medrad, Indianola, Pa) combined with a 4-channels Torso array

coil in 1.5-T MR imaging units (SignaHDxt, GE Healthcare, Milwaukee, Wis). Immediately before the MR imaging examination, all patients underwent intravascular administration of 20 mg of hyoscine-n-butylbromide (The Government Pharmaceutical Organization, Thailand) to prevent peristalsis artifacts except when contraindicated.

All patients were imaged in supine position. After the acquisition of localizing images, sagittal, coronal, axial thin-slice T2-weighted fast spin-echo (FSE) images through the prostate gland and seminal vesicles were obtained using the following parameter: TR range, 3,000 to 6,000 milliseconds; TE, 104 milliseconds; echo-train length, 18; field of view, 16x16 cm; section thickness, 3 mm; intersection gap, 0 mm; matrix 512x256; and number of excitation (NEX), 4. The transverse axial T1-weighted fast spin echo (FSE) images with a TR/TE of 400-600/10-15; matrix, 320x224; and all other parameters matched to the axial thin-sliced T2W FSE sequence were obtained. The axial thin-slice T2-weighted images were used for calculate prostatic volume by Functool package post processing with the GE advantage workstation (GE Medical Systems).

Axial free-breathing DWI was performed using a single-shot echo-planar imaging technique with a TR of 3,000-6,000 milliseconds and a TE of 60-120 milliseconds; FOV, 18x18 cm; section thickness, 5 mm; intersection gap, 1 mm; matrix 128x128; and number of excitation (NEX), 6. The axial free-breathing DTI was performed in eight patients of this study using a TR of 8,000-9,000 milliseconds and all other parameters matched to the DWI. ADC values were obtained from the DWI/DTI sequences, which were performed with b-values of 100, 250, 500, 750, 1,000, and 2,000 s/mm². The ADC maps were generated by auto-calculation the ADC value in each pixel of each slice.

Axial T1 and T2FS of the pelvis from aortic bifurcation to pubic symphysis, MR spectroscopy of the prostate gland, and axial free-breathing dynamic contrast enhanced MR images of the entire prostate gland were also obtained for all of the patients, but those images were not used in our study.

MR imaging analysis

All sequences of the MR examination of each patient were reviewed by body imaging radiologist (SP) and fellow (PW) with eight and two years of experience interpreting prostate MR examinations, respectively. The criteria for tumor visibility were focal

hyperintensity of DW images and corresponding with hypointensity on ADC maps relative to the rest of the prostate gland. The degrees of tumor visibility were recorded by using three point scales, depend on the degree of conspicuity of tumor from the remaining prostate tissue, 1 = poor; 2 = moderate; 3 = good. The locations of tumor detected by DW/DT images and ADC map and total prostatic volumes were recorded.

After a hypointense lesion of peripheral zone was identified on an ADC map, regions of interest (elliptical ROIs) were drawn manually to include the entire tumor. The mean signal intensity values and SDs in aforementioned ROI of each b-values were automatically determined by the PACS (Synapse, Fuji Medical systems). The ADC value of the areas (sides) of no detectable hypointense ADC lesion of peripheral zone were also determined by manually drawn the same size of elliptical ROIs in the same slices. In the case of pathologically proved diffuse tumor infiltration, the mean ADC values were calculated from the mean ADC value of both-sided prostate glands. The T1- and T2-weighted sequences were reviewed only to confirm findings on other sequences and to ensure that any measured areas of restricted diffusion were not interfered due to presence of blood products. The presence and locations (sides) of hypersignal T1-weighted images were also recorded.

The extracapsular extension (ECE) criteria on T2-weighted images are neurovascular bundle asymmetry, tumor envelopment of the neurovascular bundle, angulated contour of the prostate gland, irregular or spiculated margin, and obliteration of the rectoprostatic angle⁽¹⁶⁾. The seminal vesicle invasion (SVI) criteria on T2-weighted images are focal low signal intensity of the seminal vesicles, enlargement with a low-signal-intensity mass, direct tumor extension from the base to the undersurface of the seminal vesicle, and expanded low-signal-intensity ejaculatory duct with low-signal-intensity seminal vesicles⁽¹⁶⁾. The presence and locations of extracapsular extension (ECE) and seminal vesicle invasion (SVI) were also recorded.

Histopathologic analysis

A genitourinary pathologist (PC with 20 years of experience in genitourinary pathology) reviewed hematoxylin-eosin-stained slices of prostatic tissue from radical prostatectomy of all 39 patients. The locations (sides) of tumor, Gleason score, and presence and location of extracapsular extension (ECE) and seminal vesicle invasion (SVI) were determined. In

the discordant findings between radiologist and pathologist, additional pathological reviews were also recorded.

Statistical analysis

The patient data, MR imaging, and histopathologic data were summarized by tabulating mean and SD for normally distributed continuous variables, median values and ranges for asymmetrical continuous variables and tabulating percentage for categorical variables.

The K (kappa) test was used to assess agreement between histopathological and radiological results in terms of location (side) of tumor, presence and location of extracapsular extension and seminal vesicle invasion (SVI). The degrees of agreement were categorized as follows: K-values of <0.20 were considered to indicate poor agreement; K-values of 0.21-0.40, fair agreement; K-values of 0.41-0.60 moderate agreement; K-values of 0.61-0.80, good agreement; K-values of 0.81-1.00, excellent agreement⁽¹⁷⁾.

The mean ADC values in each b-value of the tumor and non-tumor were analyzed by using sign test for asymmetrical data distribution and paired t-test for normally distributed data. The mean ADC values in each b-value were also analyzed according to tumor grading; Grade I, low grade (Gleason score 1-5); Grade II, intermediate grade (Gleason score 6-7); or Grade III, high grade (8-10); by using Wilcoxon rank-sum (Mann-Whitney) test and Kruskal-Wallis equality-of population rank test. Analysis were performed by using stata version 11.1 (StataCorp 2009. Stata: Release 11. Statistical Software College Station, TX: StataCorp LP). Statistical significance was defined on the basis of p-value of less than 0.05.

Results

Patient characteristics

In this study, 39 men (mean age, 65.67 years; SD 6.23; range, 48-79 years) underwent endorectal MR imaging between March 2006 and March 2010 and subsequent radical prostatectomy with histopathologically proven adenocarcinoma of the peripheral zone of the prostate gland. The patient characteristics are described in Table 1.

MRI findings

The mean total prostatic volume of the 39 patients were 32.09 cc (SD, 13.64; range 18.59-84.85). Twenty-three (58.97%) patients had hypersignal

Table 1. Characteristic and clinical data of the patients (n = 39 patients)

Characteristic	Values
Age (years)	65.67 (SD, 6.23; range, 48-79 years)
Underlying disease	33 (84.62%)
Diabetes	13 (33.33%)
Hypertension	26 (66.67%)
Dyslipidemia	18 (46.15%)
Coronary artery disease	7 (17.95%)
Renal impairment	2 (5.13%)
Benign prostatic hyperplasia	16 (41.03%)
No underlying disease	6 (15.38%)
Serum PSA value (ng/mL, median)	14.2 (range, 3.9-179.6)
Duration after biopsy to MRI study (days, median)	70 (range 6 to 301 days)
Type of radical prostatectomy	
Open	7 (17.94%)
Laparoscopic	32 (82.05%)
Duration after MRI study to surgery (days, median)	58 (SD, 203.91; range, 4-1,271)

PSA = prostate specific antigen; MRI = magnetic resonance imaging

T1-weighted foci of hemorrhage. All of the patients in this group had hypersignal T1-weighted foci in the peripheral zone, whereas five (21.74%) patients had hypersignal T1-weighted foci in the central gland. Seventeen (73.91%) patients had hypersignal T1-weighted foci in the right lobe of prostate gland and 22 (95.65%) patients had hypersignal T1-weighted foci in the left lobe of prostate gland.

Eighteen (46.15%) patients had at least one MR imaging criteria of extracapsular extension (ECE) on T2-weighted sequence. ECE was identified on right and left sides in five (27.78%) patients each. ECE on both sides were identified in eight (44.44%) patients.

Nine (23.08%) patients had at least one MR imaging criteria of seminal vesicle invasion (SVI) on T2-weighted sequence. Unilateral seminal vesicle invasion was identified in two (22.22%) patients. Bilateral seminal vesicle invasions were identified in seven (77.78%) patients.

DWI with ADC map

Twenty-five (64.10%) patients obtained ADC map from DWI sequences, whereas 14 (35.90%) patients obtained from DTI sequences. All of the patients had b-values of 500 and 1,000 sec/mm². Eight (20.51%) patients had b-value of 100 sec/mm². Twelve (30.77%) patients had b-value of 250 sec/mm². Sixteen (41.03%) patients had b-value of 750 sec/mm². Twenty-five (64.10%) patients had b-value of 2,000 sec/mm². The mean manual elliptical ROIs of all patients were 25.60 mm³ (SD, 10.61; range 14.68 -59.81).

Two (5.13%) patients were not visible focal area of tumor by DW images with ADC map in the peripheral zone. According to a three-point scale of degree of conspicuity of tumor by DW images, 11 (28.21%) patients had grade I, eight (20.51%) patients had grade II, and 18 (46.15%) patients had grade III. Unilateral abnormality was found in 14 (35.9%) patients, seven subjects in each side. Twenty-three (58.97%) patients had a suspicious lesion involving in both lobes of peripheral zone.

Histopathologic findings and diagnosis

All of the patients in this study had adenocarcinoma of the peripheral zone of prostate gland. Two (5.13%) patients had Grade I, low grade (Gleason score 1-5). Twenty-seven (69.23%) patients had Grade II, intermediate grade (Gleason score 6-7). Ten (25.64%) patients had Grade III, high grade (8-10).

Four (10.26%) patients had tumor cell in the right lobe of peripheral zone of prostate gland. Eight (20.51%) had tumor cell in the left lobe of peripheral zone of the prostate gland. Twenty-seven (69.23%) patients had tumor cell in both lobes of peripheral zone of the prostate gland. The details are described in Table 2.

Eighteen (46.15%) patients in the study had pathologically proved focal extracapsular extension. Six (33.33%) patients in this group had focal extracapsular extension on the right side. Seven (38.89%) patients had focal extracapsular extension on the left side. Five (27.78%) patients had focal extracapsular

Discussion

In this study, there is moderate degree of agreement between DWI and histopathology in term of tumor localization and the presence and location of extracapsular extension (ECE) of peripheral zone prostate cancer. The false positive DWI results are probably due to small tumor volume, low Gleason score, and presence of prostatic hyperplasia.

In the case that presence of hypointense ADC lesions, but negative for malignancy in

histopathology, there are presence of combination of atypical adenomatous hyperplasia (AAH), prostatic intraepithelial neoplasia (PIN), benign prostatic hyperplasia (BPH), and chronic prostatitis. This could be explained by principle of DWI that assesses the Brownian motion of free water in the tissue using a pair of strong diffusion gradients⁽¹⁸⁾. The presence of small granular proliferation in atypical adenomatous hyperplasia, nuclear crowding and prominent nuclei in the glands in PIN, stromal and glandular hyperplasia in BPH, and lymphocytes aggregation in prostatitis may cause relatively restricted motion of water molecules in aforementioned areas^(19,20). False positive finding in DWI may occur in these conditions.

There were four patients with pathologically proved presence of extracapsular extension but cannot be demonstrated by T2W-images, because all of these patients have only small focal areas of ECE. Four patients were over diagnosis of ECE by T2W-images, due to over interpretation of mild capsular irregularity adjacent the suspicious tumor from fibrosis, artifact, and inflammation as the tumor invasion. There were two patients over diagnosis of SVI by T2W-images, due to presence of focal hyposignal T2W-images change adjacent to the suspicious tumor from fibrosis and inflammation.

Table 3. Apparent diffusion coefficient (ADC) values ($\times 10^{-3}$ mm²/sec) of tumor and non-tumor areas (n = 37 patients)

ADC values	n	Tumor	Non-tumor	p-value
b = 100	1	0.01	0.032	n/a
b = 250	1	1.38	2.07	n/a
b = 500	12	1.09 (SD = 0.12)	1.60 (SD = 0.16)	0.02
b = 750	5	1.08 (SD = 0.18)	1.70 (SD = 0.26)	0.19
b = 1,000	12	1.20 (SD = 0.10)	1.72 (SD = 0.14)	0.04
b = 2,000	11	1.34 (SD = 0.15)	2.01 (SD = 0.21)	0.01

Table 4. Apparent diffusion coefficient (ADC) values ($\times 10^{-3}$ mm²/sec) according to tumor grading (Gleason score)

b-value	Tumor grading						p-value
	Grade 1 (n = 2)		Grade 2* (n = 27)		Grade 3 (n = 10)		
	n	ADC value (SD)	n	ADC value (SD)	n	ADC value (SD)	
100 (n = 8)	0		6	1.68 (0.98)	2	1.33 (0.65)	0.66
250 (n = 11)	0		9	1.32 (0.40)	2	0.75 (0.45)	0.11
500 (n = 38)	2	1.59 (0.29)	26	1.22 (0.41)	10	1.12 (0.30)	0.30
			p-value = 0.62		p-value = 1.00		
			p-value = 0.38				
750 (n = 16)	2	1.66 (0.23)	7	0.99 (0.27)	7	1.10 (0.34)	0.052
			p-value = 0.052		p-value = 1.000		
			p-value = 0.12				
1,000 (n = 38)	2	1.95 (0.33)	26	1.16 (0.27)	10	1.10 (0.36)	0.0027
			p-value = 0.03		p-value = 1.00		
			p-value = 0.002				
2,000 (n = 25)	2	2.21 (0.84)	15	1.22 (0.38)	8	1.24 (0.54)	0.020
			p-value = 0.01		p-value = 1.00		
			p-value = 0.04				

* One patient with tumor grade 2 prostate cancer was excluded due to outlier data

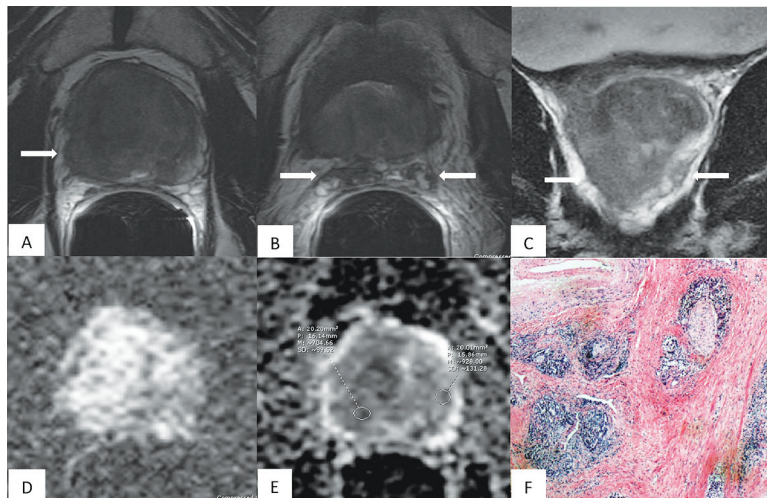


Fig. 2 A 68-year-old man, with PSA level of 49 ng/mL and Gleason score 4+3 prostate cancer involving both lobes of the prostate gland with bilateral ECE and bilateral SVI. Thin-sliced axial (A, B) and coronal (C) T2W shows diffuse hyposignal changes in both prostatic lobes with irregularity of the bilateral prostatic capsules (arrow in A, C) and hyposignal intensity of bilateral seminal vesicles (arrow in B). Diffusion-Weighted-Images (DWI) (D) with ADC map (E) at $b = 1,000 \text{ s/mm}^2$ show diffuse area of restricted diffusion. The mean ADC values calculated from ADC value on the right side, $0.70 \times 10^{-3} \text{ mm}^2/\text{sec}$ (ROI, 20.20 mm^3); and the left side $0.93 \times 10^{-3} \text{ mm}^2/\text{sec}$ (ROI, 20.01 mm^3). Note two points for tumor visibility scale in this case. The hematoxylin-eosin-stained slice of the same patient at x40 in F.

There is lower ADC value in tumor area than in the non-tumor areas in all b-values, which is corresponded to the several previous studies that compared ADC value of malignant tissue and normal prostatic tissue^(10-13,21). However, this study found statistically significant difference of ADC value between tumor and non-tumor areas only at b-value of 500, 1,000, and 2,000 sec/mm^2 , but not in other b-values. This might be due to small population and missing some data in other b-values. It also should be noted that the ADC values of non-tumor areas in this study are not representing true ADC value of the normal prostatic tissue. Because, these ADC values of non-tumor areas are measured in relative older age patient population, in which there have been developing prostatic hyperplasia, resulting in the change of ADC value⁽²²⁾.

In our study, there is negative correlation between ADC value and tumor grading in most of b-values with statistical significance at the b-value of 1,000 and 2,000 sec/mm^2 between tumor grade I and tumor grade II, and between tumor grade I and III. These results are corresponding with the several previous studies that demonstrate high-grade tumors tending to show lower ADC values^(21,23-25). Possible explanations to this could be increased tumor cellularity, structural change of gland stroma that

becomes more fibrous, and a more disorganized texture resulting in a relatively more restricted motion of water molecules within high-grade tumors.

Conversely, there is relatively low ADC value of tumor grade II than grade III at the b-values of 750 and 2,000 sec/mm^2 , probably due to disproportional number of patients between tumor grade II (69.23%) and tumor grade III (25.64%) and heterogeneity data of the ADC values in the same group. In addition, prostate cancer is frequently described as histologically heterogeneous and more than 50% of patients with prostatic cancer have at least three different Gleason grades^(26,27).

Our study had several limitations. First, it was a retrospective study with a relatively small sample size, which could be influenced by selection and verification biases. In addition, there was disproportional number of patients in different tumor grading, the relationship between tumor grading and ADC values may therefore be weak. Larger prospectively studied patient population will be needed to refine the cutoff values, proper b-values, and the relationship between ADCs and tumor aggressiveness. Third, the radiologist was not blinded to histopathological findings when assessing ADC maps. Finally, the slice level in MR images cannot be matched exactly with that of histopathology, only side (lobe) of prostate gland was compared.

In conclusion, the study suggested that tumor show low ADC value than non-tumor areas at all b-values with statistical significance at b-value 500, 1,000, and 2,000 sec/mm². The ADC values showed a negative correlation between low and intermediate grades and between low and high grades tumor at the b = 1,000 and 2,000 sec/mm². DWI with ADC maps may be a useful tool for noninvasive assessment of the aggressiveness of prostate cancers that are visible on MR images.

Potential conflicts of interest

None.

References

- Ramathibodi cancer report 2008. Bangkok: Faculty of Medicine, Ramathibodi Hospital Mahidol University; 2008.
- Attasara P, Buasom R. Hospital-based cancer registry. Bangkok: National Cancer Institute Department of Medical Services Ministry of Public Health; 2009.
- McKenna DA, Coakley FV, Westphalen AC, Zhao S, Lu Y, Webb EM, et al. Prostate cancer: role of pretreatment MR in predicting outcome after external-beam radiation therapy—initial experience. *Radiology* 2008; 247: 141-6.
- Woodfield CA, Tung GA, Grand DJ, Pezzullo JA, Machan JT, Renzulli JF. Diffusion-weighted MRI of peripheral zone prostate cancer: comparison of tumor apparent diffusion coefficient with Gleason score and percentage of tumor on core biopsy. *AJR Am J Roentgenol* 2010; 194: W316-22.
- Lim HK, Kim JK, Kim KA, Cho KS. Prostate cancer: apparent diffusion coefficient map with T2-weighted images for detection—a multireader study. *Radiology* 2009; 250: 145-51.
- Yoshimitsu K, Kiyoshima K, Irie H, Tajima T, Asayama Y, Hirakawa M, et al. Usefulness of apparent diffusion coefficient map in diagnosing prostate carcinoma: correlation with stepwise histopathology. *J Magn Reson Imaging* 2008; 27: 132-9.
- Kim CK, Park BK, Han JJ, Kang TW, Lee HM. Diffusion-weighted imaging of the prostate at 3 T for differentiation of malignant and benign tissue in transition and peripheral zones: preliminary results. *J Comput Assist Tomogr* 2007; 31: 449-54.
- Turkbey B, Pinto PA, Choyke PL. Imaging techniques for prostate cancer: implications for focal therapy. *Nat Rev Urol* 2009; 6: 191-203.
- van As NJ, de Souza NM, Riches SF, Morgan VA, Sohaib SA, Dearnaley DP, et al. A study of diffusion-weighted magnetic resonance imaging in men with untreated localised prostate cancer on active surveillance. *Eur Urol* 2009; 56: 981-7.
- Pickles MD, Gibbs P, Sreenivas M, Turnbull LW. Diffusion-weighted imaging of normal and malignant prostate tissue at 3.0T. *J Magn Reson Imaging* 2006; 23: 130-4.
- Kumar V, Jagannathan NR, Kumar R, Thulkar S, Gupta SD, Dwivedi SN, et al. Apparent diffusion coefficient of the prostate in men prior to biopsy: determination of a cut-off value to predict malignancy of the peripheral zone. *NMR Biomed* 2007; 20: 505-11.
- deSouza NM, Reinsberg SA, Scurr ED, Brewster JM, Payne GS. Magnetic resonance imaging in prostate cancer: the value of apparent diffusion coefficients for identifying malignant nodules. *Br J Radiol* 2007; 80: 90-5.
- Wang X, Ding J, Jiang X. Diffusion-weighted MR imaging of seminal vesicle and prostate gland in normal volunteers. *Proc Intl Soc Mag Reson Med* 2004; 11: 938.
- Egevad L, Granfors T, Karlberg L, Bergh A, Stattin P. Prognostic value of the Gleason score in prostate cancer. *BJU Int* 2002; 89: 538-42.
- Bianco FJ Jr, Wood DP Jr, Cher ML, Powell IJ, Souza JW, Pontes JE. Ten-year survival after radical prostatectomy: specimen Gleason score is the predictor in organ-confined prostate cancer. *Clin Prostate Cancer* 2003; 1: 242-7.
- Claus FG, Hricak H, Hattery RR. Pretreatment evaluation of prostate cancer: role of MR imaging and 1H MR spectroscopy. *Radiographics* 2004; 24 (Suppl 1): S167-80.
- Bammer R. Basic principles of diffusion-weighted imaging. *Eur J Radiol* 2003; 45: 169-84.
- Doll JA, Zhu X, Furman J, Kaleem Z, Torres C, Humphrey PA, et al. Genetic analysis of prostatic atypical adenomatous hyperplasia (adenosis). *Am J Pathol* 1999; 155: 967-71.
- Miller GJ, Torkko KC. Natural history of prostate cancer—epidemiologic considerations. *Epidemiol Rev* 2001; 23: 14-8.
- Tamada T, Sone T, Jo Y, Toshimitsu S, Yamashita T, Yamamoto A, et al. Apparent diffusion coefficient values in peripheral and transition zones of the prostate: comparison between normal and malignant prostatic tissues and correlation with histologic grade. *J Magn Reson Imaging*

- 2008; 28: 720-6.
21. Tamada T, Sone T, Toshimitsu S, Imai S, Jo Y, Yoshida K, et al. Age-related and zonal anatomical changes of apparent diffusion coefficient values in normal human prostatic tissues. *J Magn Reson Imaging* 2008; 27: 552-6.
 22. Itou Y, Nakanishi K, Narumi Y, Nishizawa Y, Tsukuma H. Clinical utility of apparent diffusion coefficient (ADC) values in patients with prostate cancer: can ADC values contribute to assess the aggressiveness of prostate cancer? *J Magn Reson Imaging* 2011; 33: 167-72.
 23. Turkbey B, Shah VP, Pang Y, Bernardo M, Xu S, Kruecker J, et al. Is apparent diffusion coefficient associated with clinical risk scores for prostate cancers that are visible on 3-T MR images? *Radiology* 2011; 258: 488-95.
 24. deSouza NM, Riches SF, Vanas NJ, Morgan VA, Ashley SA, Fisher C, et al. Diffusion-weighted magnetic resonance imaging: a potential non-invasive marker of tumour aggressiveness in localized prostate cancer. *Clin Radiol* 2008; 63: 774-82.
 25. McNeal JE, Villers AA, Redwine EA, Freiha FS, Stamey TA. Histologic differentiation, cancer volume, and pelvic lymph node metastasis in adenocarcinoma of the prostate. *Cancer* 1990; 66: 1225-33.
 26. Aihara M, Wheeler TM, Ohori M, Scardino PT. Heterogeneity of prostate cancer in radical prostatectomy specimens. *Urology* 1994; 43: 60-6.

ประโยชน์ทางคลินิกของการตรวจการเคลื่อนที่ของโมเลกุลน้ำด้วยการตรวจเอกซเรย์ด้วยคลื่นแม่เหล็กไฟฟ้าในผู้ป่วยมะเร็งต่อมลูกหมาก

พรพรรณ วิบูลผลประเสริฐ, สิทธิ พงษ์กิจการุณ, พันธ์ เฉลิมแสนยากร

วัตถุประสงค์: เพื่อระบุความสัมพันธ์ของค่า *apparent diffusion coefficient (ADC)* ที่ได้จากการตรวจเอกซเรย์ด้วยคลื่นแม่เหล็กไฟฟ้าบริเวณต่อมลูกหมากในค่า *b-values* ที่ต่างกัน และระดับความรุนแรงของเนื้องอกตาม *Gleason score* ของมะเร็งต่อมลูกหมากบริเวณ *peripheral zone (PZ)*

วัสดุและวิธีการ: เป็นการศึกษาย้อนหลังในผู้ป่วยมะเร็งต่อมลูกหมากบริเวณ *PZ* จำนวน 39 ราย ที่ได้รับการตรวจ *endorectal diffusion-weighted (DW) magnetic resonance imaging (MRI)* ก่อนการผ่าตัดต่อมลูกหมากชนิด *radical prostatectomy* ในช่วง เดือนมีนาคม พ.ศ. 2549 ถึง เดือนมีนาคม พ.ศ. 2553 โดยเปรียบเทียบค่า *ADC* ในบริเวณเนื้องอกและบริเวณที่ไม่มีเนื้องอกที่ค่า *b = 100, 250, 500, 750, 1,000, และ 2,000 sec/mm²* โดยใช้ *paired t-test and sign-test* และหาความสัมพันธ์ระหว่างค่า *ADC* และระดับความรุนแรงของเนื้องอก

ผลการศึกษา: ค่าเฉลี่ย *ADC* บริเวณเนื้องอกจะต่ำกว่าบริเวณที่ไม่มีเนื้องอกในทุกค่า *b-values* อย่างมีนัยสำคัญทางสถิติ และมี *negative correlation* ระหว่างค่า *ADC* และระดับความรุนแรงของเนื้องอกที่ *b = 1,000 sec/mm²* ระหว่างเนื้องอกระดับ 1 ($1.95 \times 10^{-3} \text{ mm}^2/\text{sec}$, $SD = 0.33$) กับเนื้องอกระดับ 2 ($1.16 \times 10^{-3} \text{ mm}^2/\text{sec}$, $SD = 0.27$) ($p = 0.03$) และระหว่างเนื้องอกระดับ 1 กับเนื้องอกระดับ 3 ($1.10 \times 10^{-3} \text{ mm}^2/\text{sec}$, $SD = 0.36$) ($p = 0.002$), และที่ *b = 2,000 sec/mm²*, ระหว่างเนื้องอกระดับ 1 ($2.21 \times 10^{-3} \text{ mm}^2/\text{sec}$, $SD = 0.08$) กับเนื้องอกระดับ 2 ($1.22 \times 10^{-3} \text{ mm}^2/\text{sec}$, $SD = 0.38$) ($p = 0.01$), และระหว่างเนื้องอกระดับ 1 กับเนื้องอกระดับ 3 ($1.32 \times 10^{-3} \text{ mm}^2/\text{sec}$, $SD = 0.49$) ($p = 0.04$) ในขณะที่ค่า *ADC* ระหว่างเนื้องอกระดับ 2 และ 3 ไม่แตกต่างกันในทุกค่า *b-values*

สรุป: บริเวณเนื้องอกจะมีการเคลื่อนที่ของโมเลกุลน้ำลดลง ทำให้มีค่า *ADC* ต่ำกว่าบริเวณที่ไม่มีเนื้องอก โดยมี *negative correlation* ระหว่างค่า *ADC* และระดับความรุนแรงของเนื้องอกที่ *b = 1,000 และ 2,000 sec/mm²* ดังนั้นการวัดค่า *ADC values* อาจจะเป็นเครื่องมือในการประเมินความรุนแรงของมะเร็งต่อมลูกหมากที่พบได้จากการตรวจเอกซเรย์ด้วยคลื่นแม่เหล็กไฟฟ้า